THE INTERACTION BETWEEN THE OUTFLOW OF TYPHOON JANGMI (2008)
AND THE MIDLATITUDE JET DURING T-PARC

Christian M. Grams *
Karlsruhe Institute of Technology, Karlsruhe, Germany

1. INTRODUCTION

The presence of a tropical cyclone undergoing extratropical transition (ET) is accompanied by low predictability for the Atlantic-European and Northwest-American sector (Harr et al., 2008; Anwender et al., 2008). In a number of recent case studies of ET the excitation of a characteristic pattern has been identified, consisting of an upstream trough, a downstream ridge and a second trough further downstream (Rossby Wave Train, RWT), which may trigger high-impact weather in the midlatitudes (Riemer et al., 2008). The investigation of the mechanisms by which an ET event influences the downstream predictability was one of the primary objectives of the THORPEX Pacific Asian Regional Campaign (T-PARC) in 2008. During T-PARC the outflow of Typhoon Jangmi showed a distinct interaction with the midlatitude jet stream. As the typhoon approached the midlatitudes the jet expanded further south and the wind speed in the jet core increased. Although this case does not fit in the classical view of ET and the triggering of a RWT described above it gives insight into the variety of interactions between tropical and extratropical weather systems which may occur during ET. This study is based on model output from the COSMO model (Consortium for Small-scale Modeling[1]). We use potential vorticity inversion to quantify the impact of Jangmi on the midlatitude flow.

2. DATA AND METHODS

2.1 *The COSMO Model*

COSMO is a non-hydrostatic regional numerical weather prediction model designed for the meso-β (5-50km) and meso-γ (500m-5km) scale (Steppeler et al., 2003; Schättler et al., 2009). The non-hydrostatic thermo-hydrodynamical equations for compressible flow are formulated on a rotated geographical coordinate system, using an Arakawa-C grid. In the vertical a hybrid vertical coordinate is used, terrain following in the lower half of the troposphere. In this study we do not use a rotated grid as the region of interest is close to the equator. The vertical layers were defined to be as close as possible to the vertical layers of the input fields. The basic equations are solved using the time-splitting technique of Klemp and Wilhelmson (1978). The various physics package of COSMO include a turbulence and surface layer scheme using a prognostic turbulent kinetic energy equation with a 2.5 order closure by Mellor and Yamada (1982) with extensions by Raschendorfer (2001) and a two-category bulk model cloud microphysics scheme (Doms and Schättler, 2002; Gaßmann, 2002). Precipitation formation is treated by a Kessler-type bulk microphysics parametrization (Kessler, 1969) including water vapor, cloud water, rain and cloud ice with column equilibrium for the precipitating phase. The subgridscale clouds, on the other hand, are parametrized by an empirical function depending on relative humidity and height. A δ twostream radiation scheme (Ritter and Geleyn, 1992) is used for the short- and longwave fluxes and the full cloud radiation feedback. The surface layer is parametrized by a stabilitydependent draglaw formulation of momentum, heat and moisture fluxes according to similarity theory.

The data basis of this study is a reference data set which we produced from the ECMWF (European Centre for Medium-Range Weather Forecasts) IFS analyses (Integrated Forecast System) and which we call the COSMO pseudo analysis. This data set consists of 6 hourly COSMO runs at 0.25° horizontal resolution initialized every 6 hours from 6 hourly IFS analyses. One hourly model output of the individual 6 hour forecasts is combined to cover the period 00 UTC 27 September 2008 to 23 UTC 03 October 2008. Thus every 6 hours the pseudo analysis is the IFS analysis interpolated on the COSMO grid. The COSMO pseudo analysis serves as the initial and boundary data for further model runs.

2.2 *Potential Vorticity Inversion*

Potential vorticity (PV) (Ertel, 1942) is a key quantity for the investigation of ET. PV is conserved following three-dimensional, adiabatic and inviscid motion. When the flow is not adiabatic, for example in regions of latent heat release, changes in PV can be related to the spatial distribution of the diabatic heating or cooling. Different features involved in the ET process can easily be determined by their characteristic PV structure and the conservation principle allows them to be tracked. The core of a tropical cyclone constitutes a strong positive PV anomaly. Above the storm, a region of low or negative PV characterizes the outflow region. During ET, latent heat release due to condensation in the warm sector leads to a secondary positive PV anomaly at lower levels. At upper levels a sharp PV gradient with high (stratospheric) values at the poleward side marks the transition to the midlatitudes. This is where the jet stream occurs and deflections result in upper tropospheric troughs (positive PV anomaly) and ridges (negative PV anomaly) a so-called Rossby wave train (RWT). In this study PV is calculated from the

---

Corresponding author address: Christian Grams, Karlsruhe Institute of Technology, Institute for Meteorology and Climate Research, 76128 Karlsruhe, Germany; e-mail: grams@kit.edu
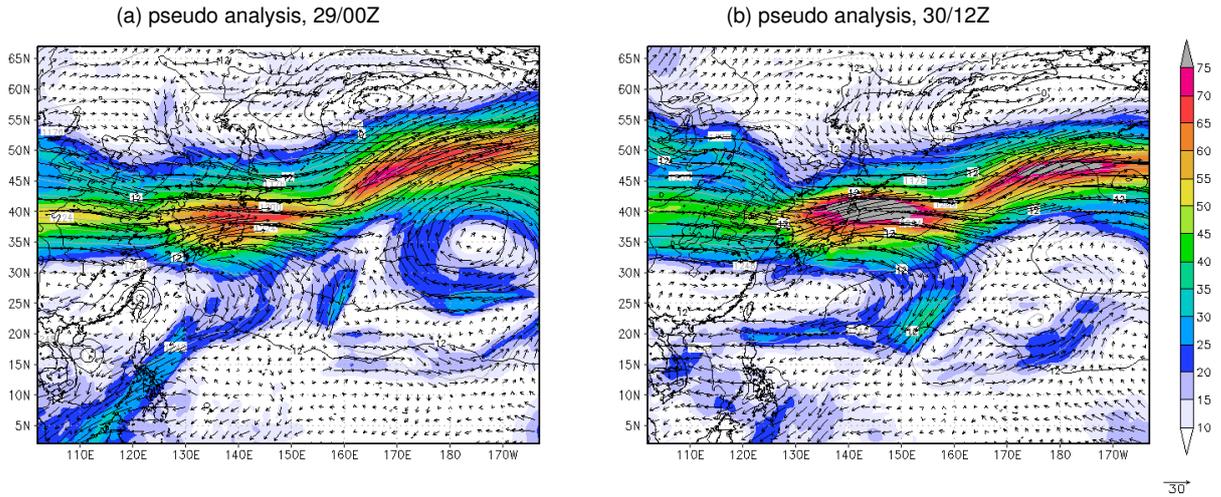
[1] http://www.cosmo-model.org/

FIG. 1: Wind vectors (black), wind speed (shaded, with a 5ms^{-1} contour interval starting at 10ms^{-1}) at 200hPa, and geopotential at 1000 hPa (black contours, with a 4 gpdm contour interval), at 00UTC 29 September 2008 (left) and 12UTC 30 September 2008 (right). Data from 0.25° COSMO pseudo analysis.

COSMO model fields.

Using the invertibility principle of PV it is possible to calculate the flow and temperature field - the "balanced fields" - associated with the PV field. We use an algorithm (Davis and Emanuel, 1991; Davis, 1992) which assumes non-linear balance (Charney, 1955).

The balanced geopotential, wind, and temperature fields from the PV inversion are used along with modified fields of humidity and vertical velocity as initial fields for a new COSMO run. In a first step PV inversion is effected on the original PV field and a new model run – the control run (CNTRL) – is initialized from the balanced fields. In a second step the tropical cyclone is removed from the PV field of the same domain, a PV inversion is effected, and the new balanced fields without the tropical cyclone are used as initial fields for a new model run – the NOTC run. Extracting the tropical storm at a time before interaction with the midlatitude flow occurs allows us to study the impact of the tropical storm on the midlatitude flow. This method of using the balanced fields of PV inversion as initial data for a new model run is very similar to the method used in the studies on the ET of Hurricane Irene (1999) and Tropical Strom Lili (1996) by (Agustí-Panareda et al., 2004; Agustí-Panareda et al., 2005).

2.3 *Modification of the PV and moisture fields*

The PV field is modified by defining a box around the PV-anomaly and setting the PV at each grid point to a critical value where it exceeds (in the case of removing a positive PV anomaly) or undercuts (in the case of removing a negative PV anomaly) this threshold. The critical value is defined for each level as the spatial average PV of the level. The domain averaged PV is kept constant by distributing the sum of the PV removed to all grid points of the level.

In some runs the moisture anomaly is modified also. A rectangular box in geographical and model level coordinates is defined around the storm and within the box the specific humidity, specific cloud ice content and specific cloud water content are set to the spatial average of that level multiplied by a factor q_f. Finally, the vertical velocity can be set to zero in the moisture modification domain.

In the case study presented in this paper, the balanced fields were computed on a domain which extends from 111-194°E, 16-60°N, 900-25 hPa and at 00 UTC 28 September 2008. The input data for the PV inversion is the COSMO pseudo analysis interpolated on pressure levels with a regular vertical grid spacing of 25 hPa. For the NOTC run the positive PV anomaly associated with Jangmi is removed in a box around the storm which covers 118-127°E, 18-26°N, and 900-100 hPa. The moisture fields were modified in the box which covers major parts of the region which was affected by advection of humidity through Jangmi (115-150°E, 17-31°N, and on all model levels, q_f = 1.4). The initial vertical velocity was set to zero within that box. Six-hourly COSMO pseudo-analyses at 0.25° horizontal resolution (thus the IFS analyses interpolated on the COSMO grid) were used as boundary data.

3. THE EXTRATROPICAL TRANSITION OF JANGMI

Super Typhoon Jangmi was a major tropical cyclone reaching category 4 on the Saffir-Simpson scale. It formed in the Philippine Sea on 24 September 2008 and while intensifying headed northwestwards towards Taiwan. The minimum central pressure was 905 hPa and the maximum surface wind speed reached more than 210 $km\,h^{-1}$. On 28 September 2008 Jangmi made landfall at the northeastern tip of Taiwan. After landfall
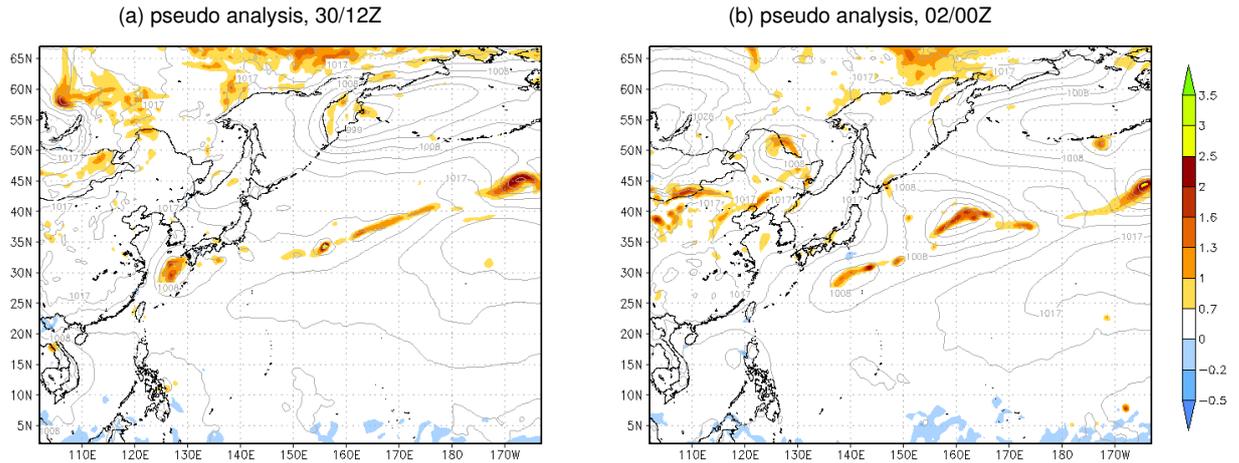
FIG. 2: Potential vorticity (shaded, in PVU) vertically averaged from 975-800 hPa, pressure at mean sea level (grey contours with a 3hPa contour interval), at 12 UTC 30 September 2008 (left) and 00 UTC 02 October 2008 (right). Data from 0.25°COSMO pseudo analysis.

the typhoon soon weakened and the structural changes indicated its transformation in an extratropical system. Jangmi recurved in the East China Sea and passed south of Kyushu before it decayed.

3.1 *Synoptic Overview*

As Jangmi approached the midlatitudes a maximum of the jet stream which was located across the northern part of Honshu became rather stationary from around 18 UTC 28 September 2008 to 18 UTC 30 September 2008. The jet streak extended southwards and a strong increase in maximum wind speed occurred. This is illustrated with the wind field at 200hPa for two time steps (Figure 1). At 00 UTC 29 September 2008 westerly flow north of 36°N indicates a zonally-oriented jet (Figure 1a) with maximum wind speed of more than 65 ms^{-1} over northern Honshu. The recurving tropical cyclone is located north of Taiwan. North of the typhoon the anticyclonic outflow of Jangmi is evident as southwesterly flow towards the jet. 36 hours later the typhoon outflow merged with a southwestward extension of the jet core and it appears that the southwesterly outflow extends into the jet core (Figure 1b). At this time the wind speed in a wide region of the jet core increased to more than $75ms^{-1}$.

The decay of Jangmi and an extratropical cyclogenesis downstream is illustrated using the low level PV average from 975 hPa to 800 hPa (Figure 2). At 12 UTC 30 September 2008 the decaying tropical storm is located southwest of Japan (Figure 2a). To the west a low level trough is indicated by the contours of mean sea level pressure. At 34°N, 141°E a closed isobar of 1011 hPa and a small region of $q > 0.7PVU$ marks the start of an extratropical cyclogenesis downstream of Jangmi. After 36 hours this extratropical low shows a clear wave signature in the low level average PV and it deepened to

999 hPa in the center. The remnants of Jangmi are located as a band of PV at around 30°N, 140°E and the isobars show a low level trough which links Jangmi to the new cyclone downstream.
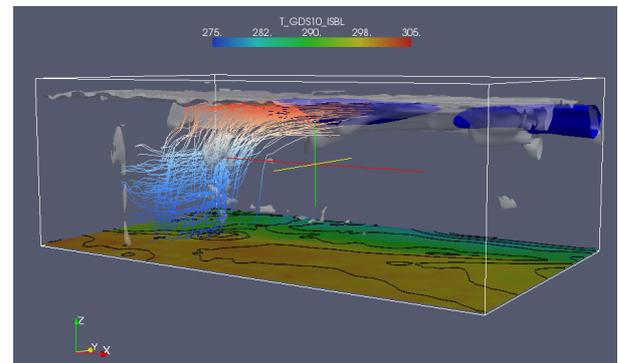

FIG. 3: Contour of potential vorticity at 2PVU (grey shaded). The transparent blue contour indicates the midlatitude jet ($|\vec{v}_h| > 60\,m\,s^{-1}$). Potential temperature in K and contours of geopotential (with a 250 gpm contour interval) are shown at 990hPa. The lines indicate 36h backward trajectories calculated from a box (130-155°E, 34-44°N, 8000-15000m amsl) in the jet core region at 12UTC 30 September 2008. The criterion for trajectory calculations is ascent>5000m. Blue-red contour shading indicates the height. Every 100th trajectory is plotted. View is from the southeast. The domain covers 110-179°E, 11-51°N and 1000-50 hPa. Data are taken from 0.25° COSMO pseudo analysis and shown at 12 UTC 30 September 2008.

3.2 *The Outflow-Jet Interaction*

Backward trajectories calculated with the LAGRANTO trajectory model (Wernli and Davies, 1997; Wernli, 1997), for a 36h time interval and starting in a box in the jet core show that Jangmi advects tropical air from mid and lower levels into the jet core (Figure 3). Trajectory calculations also indicate that the zonal flow over the Yellow Sea is deflected into the jet (not shown). The temporal evolution of the trajectories indicates that most of the lifting occurs in a broad region at the baroclinic zone which is indicated by a strong gradient of virtual potential temperature at 1000hPa (at the sharp transition from red to green). At an early stage, trajectories at all levels show that parcels are advected northward cyclonically around the PV tower associated with the core of Jangmi (seen as the westmost trajectories in Figure 3). At this time vertical motion is weak. Later, when the air parcels reached the baroclinic zone, strong ascent occurs especially for the lowest parcels (almost vertical trajectories in 3). This ascent is almost entirely confined to the region at the baroclinic zone where a new PV anomaly evolves. The air parcels continue their ascent and move towards the jet core. At 12 UTC 30 September 2008 (Figure 3) all trajectories reached the jet core. Note that there are three distinct paths into the jet core. Firstly, the early air reaching jet level is from the mid levels (above 500 hPa) and is lifted in the vicinity of the PV tower associated with the TC core. Secondly, ascent at the baroclinic zone enables lifting of air from mid levels (below 500 hPa) and low levels to the jet level. Thirdly, further air reaches the lower jet level through gradual upgliding along (moist) isentropes. The new PV at the baroclinic zone must be diabatically forced from strong latent heat release. Satellite imagery indicates new deep clouds at the baroclinic zone from around 12 UTC 30 September 2008 whereas convection in the typhoon region had almost collapsed earlier (not shown). In the following hours the new PV shows a propagation along the low level baroclinic zone which has characteristics of a diabatic Rossby wave. An extratropical cyclogenesis occurs but a strong intensification does not occur due to the lack of upper level forcing.

The isentropic PV at $\Theta = 315\,K$ shows the center of Jangmi located at around $29^{o}N, 125^{o}E$ (Figure 4). However, other PV features in the vicinity of Jangmi and the baroclinic zone are striking, namely the PV center at around $33^{o}N, 127^{o}E$ which reflects the new PV seen in Figure 3 and to the east a band of high PV at $34^{o}N, 127\text{-}136^{o}E$ where Jangmi advects warm moist air from the south towards the baroclinic zone. This is the region where warm frontogenesis occurs, as indicated by the high cloud tops of satellite imagery (not shown). The new PV and the ascent at the baroclinic zone become evident in a cross section towards the jet through Jangmi's core (Figure 5). The remnants of the TC core can be identified as a region of $q > 2PVU$ at around 500km (Figure 5a). The strong gradient of equivalent potential temperature Θ_e at 1000km indicates the baroclinic zone, that has only a small poleward tilt up to 600 hPa. The new PV

evolves directly on the equatorward side of the baroclinic zone and is maximized at 1000 km, 700 hPa. Here Θ_e is neutrally stratified and thus enables fast pseudo-adiabatic ascent into the jet level as indicated by the wind vectors in the plane of section (see also the trajectories in Figure 3). Above 500 hPa and north of 1500 km the moist isentropes (which here almost coincide with dry isentropes, not shown) are directed into the jet core and thus enable (moist) isentropic upgliding directly into the jet core. The latter is located approximately at the step of the dynamic tropopause ($q = 2PVU$) at 2100km (see also the contours of wind speed across the section in Figure 5b). At jet level the flow is almost along the isentropes. As isentropes become denser towards the jet core the flow has to accelerate. This may explain the increase in jet core wind speed. The low PV values from 400 to 200 hPa and 1300-1500km reflect the negative PV anomaly associated with the outflow. The tongue of moist air in Figure 5b between 500-300 hPa and 1300-1900km indicates the advection of tropical air towards the jet core.

4. QUANTIFICATION OF THE IMPACT OF JANGMI ON THE MIDLATITUDES USING PV INVERSION

The description of the extratropical transition of Typhoon Jangmi in the previous sections raises the question as to what extent Jangmi had an impact on the strength of the midlatitude jet and whether Jangmi triggered the extratropical cyclogenesis downstream. The PV inversion technique described in section 2.2 enables to quantify Jangmi's contribution to the total flow.

Here we show results from a CNTRL and NOTC run which were initialized from the balanced fields of the PV inversion at 00 UTC 28 September 2008. The forecasts were computed for 126 hours and 6 hourly COSMO pseudo analyses serve as boundary data. The initializa-
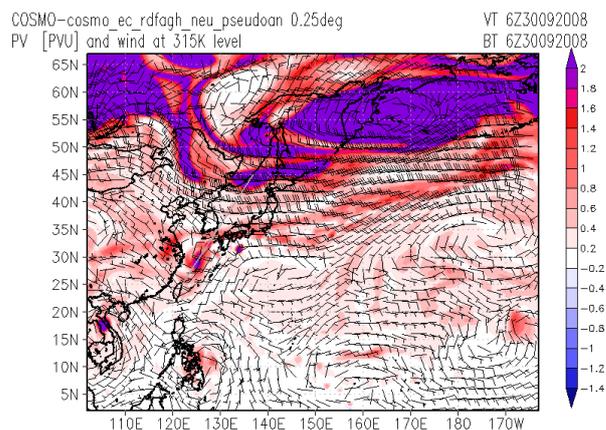

Fig. 4: Potential Vorticity (shaded) [PVU] and wind barbs at $\Theta = 315\,K$ at 06 UTC 30 September 2008. The grey line indicates the location of the cross sections in Figure 5. Data from 0.25^{o} COSMO pseudo analysis. Note the different scaling for positive and negative PV.

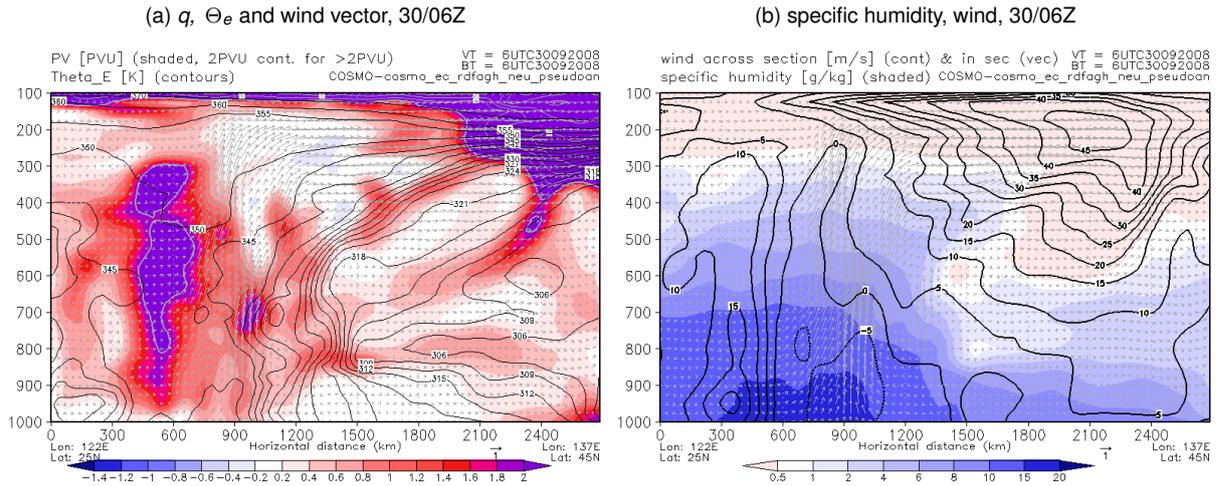(a) q, Θ_e and wind vector, 30/06Z   (b) specific humidity, wind, 30/06Z

FIG. 5: Vertical cross sections from 25°N,122°E to 45°N,137°E at 06 UTC 30 September 2008. Left: potential vorticity (shaded, with a 0.2 PVU contour interval), equivalent potential temperature (black contours, with a 3K contour interval), and wind in the plane of section (grey arrows). Right: specific humidity (shaded in g kg-1), wind across the plane of section (black contours, with a 5 ms-1 contour interval), and wind in the plane of section (grey arrows). Data from 0.25° COSMO pseudo analysis. Note the different scaling for positive and negative PV.

tion time (and the time for PV inversion) is chosen so that the midlatitude jet did not yet show an intensification and Jangmi is still located far from the midlatitudes. A verification of the CNTRL run against the pseudo analysis showed that the recurvature of Jangmi and the evolution of the midlatitude jet is represented accurately (not shown). However, after recurvature Jangmi is located further to the north than in the analysis and Jangmi itself
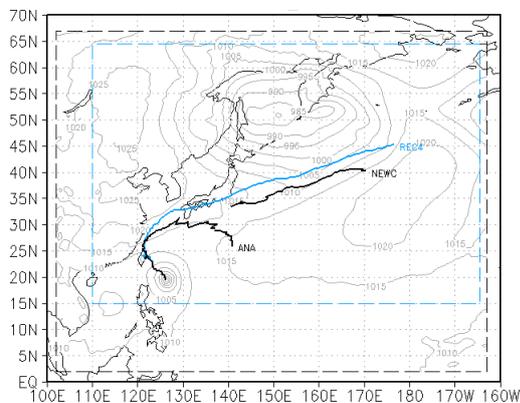

FIG. 6: Track of Jangmi (ANA, starting at 00 UTC 27 September 2008; REC4 starting at 00 UTC 28 September 2008) and the extratropical low (NEWC) in the CNTRL run (blue) and COSMO pseudo analysis (black). Note that in the CNTRL run Jangmi and the extratropical low are identical and thus only one track is shown. The dashed line marks the model region of the CNTRL run (blue) and COSMO pseudo analysis (black).
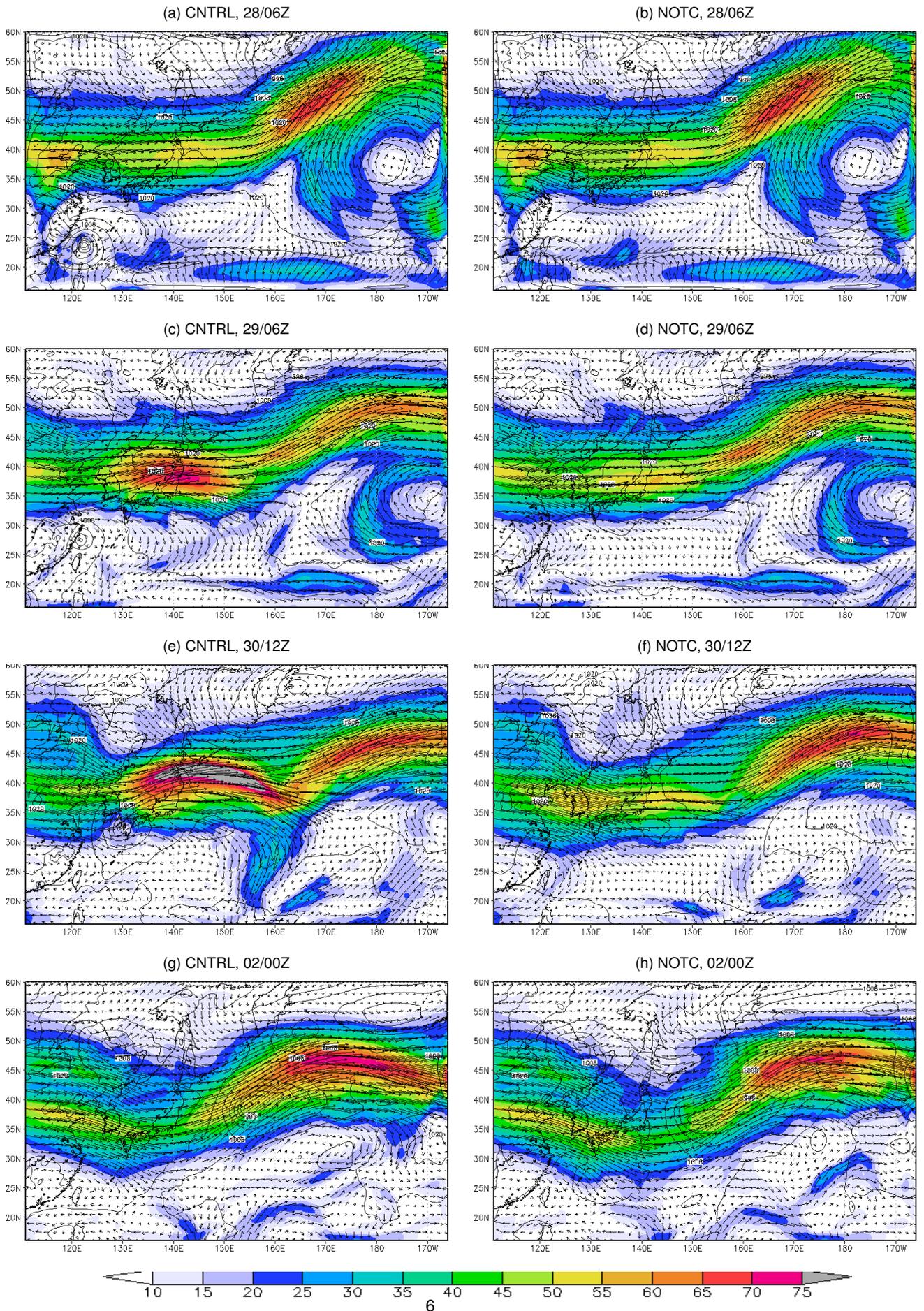
becomes an extratropical reintensifying cyclone (Figure 6, Figures 1 and 7, Figures 2 and 8). Nevertheless we found this CNTRL run together with the NOTC run to be useful for the quantification of the impact of Jangmi on the midlatitudes.

The impact of the outflow of Jangmi on the midlatitude jet becomes evident when looking at the temporal evolution of the 200 hPa wind field of the CNTRL and NOTC run (Figure 7). At 06 UTC 28 September 2008 there are hardly any differences in the upper level midlatitude flow of both runs (Figures 7a,b). A trough with its axis over northern Japan is evident and a jet streak with wind speed up to $60 ms^{-1}$ approaches from the west at 38°N. The main differences are in the vicinity of Jangmi due to the lack of the upper level outflow in the NOTC run. One day later in the CNTRL run as well as in the COSMO pseudo analysis (see Figure 1a) this jet streak becomes stationary over Japan (Figures 7c,d). The jet core wind speed in the CNTRL run reaches more than $70\ ms^{-1}$ and is much higher than in the NOTC run where it reaches only $55\ ms^{-1}$. At 12 UTC 30 September 2008 the outflow of Jangmi is directed straight into the jet core (Figures 7e,f; see also Figure 1b). In the CNTRL run the jet core wind speed downstream of Jangmi increased to more than $75 ms^{-1}$ over a large region (Figure 7e). The jet streak in the CNTRL run is located further north than in the NOTC run at around 42°N. A weak ridge evolved downstream of Jangmi over Japan. In the NOTC run the jet streak is located over Japan at around 37°N and much weaker with wind speed exceeding $60 ms^{-1}$ only in a small region (Figure 7f).

FIG. 7: Wind vectors (black), wind speed (shaded, with a $5\,\mathrm{ms}^{-1}$ contour interval starting at $10\mathrm{ms}^{-1}$) at 200hPa, and pressure at mean sea level (black contours, with a 4 hPa contour interval), at 06 UTC 28 September 2008 (top), 06 UTC 29 September 2008 (2nd row), 12 UTC 30 September 2008 (3rd row), and 00 UTC 02 October 2008 (bottom). Data in the left column is from CNTRL run, data in the right column is from NOTC run.

A rather weak trough is evident over Japan than a ridge west of Japan like in CNTRL. Further an upper level low pressure system is located at 21°N, 160°E. The cyclonic flow around this system and the flow at the eastern side of the subtropical high south of Japan is much stronger in the CNTRL run (between 20-33°N,153-165°E). 36 hours later the midlatitude upper level flow looks similar in the CNTRL and NOTC run (Figures 7g,h). The jet streak moved over the Pacific and is located at around 46°N, 165-180°E with similar position in both runs. The jet core wind speed is only slightly lower in the NOTC run than in the CNTRL run. However, there are major differences in the region of the subtropical anticyclone (e.g. 27°N, 175°E). The contours of mean sea level pressure show the reintensification of Jangmi in the CNTRL run and an extratropical cyclogenesis in the NOTC run located at the south-western edge of the jet entrance. Finally, the reintensification of Jangmi and downstream cyclogenesis is illustrated using the field of low level PV (Figure 8). The removal of Jangmi from the NOTC run using PV surgery can be seen when comparing the beginning of the CNTRL and NOTC runs and is exemplarily shown at 12 UTC 30 September 2008 (Figures 8a,b). In the CNTRL run Jangmi is located at around 33°N, 130°E while it is removed in the NOTC run. Despite this there are only minor differences in the representation of the large scale features like the central low over Kamchatka and the anticyclone over the Pacific in the first 60 forecast hours of the CNTRL and NOTC run. The PV features seen in the vicinity of Japan are not yet linked to the extratropical cyclogenesis which starts in the following hours. At 02 UTC 1 October 2008 an extratropical cyclone is present at a similar location in both the CNTRL and in the NOTC run (Figures 8c,d). In the CNTRL run Jangmi reintensified and its central pressure deepend to less than 990 hPa. In the NOTC run an extratropical cyclogenesis occurred with an elongated cyclone and a central pressure of less than 996 hPa. In addition, PV reaches higher values in the CNTRL run than in the NOTC run. The location of the cyclone in both runs is similar to the extratropical cyclone in the COSMO pseudo analysis (Figure 2a). However, the latter only reached a central pressure of about 999 hPa. Nevertheless, one has to keep in mind that at this time we analyze a 96 hour forecast. The representation of weather systems upstream of Jangmi in the analysis, CNTRL and NOTC run (e.g. the low pressure system over northeast China) is quite similar and this supports the conclusions from the comparison of the CNTRL and NOTC run.

In summary the PV surgery showed that Jangmi accelerated and deflected the midlatitude jet significantly. Furthermore, the outflow of Jangmi together with the midlatitude jet seem to accelerate the flow around the subtropical anticyclone and thus to modify the flow in the subtropics. The low level fields of PV and mean sea level pressure showed that the extratropical cyclogenesis occurred even if Jangmi is removed from the initial conditions. Thus Jangmi does not seem to trigger a development downstream. Nevertheless the extratropical cyclone is more intense when Jangmi is present in the initial conditions.

5. SUMMARY

In this study COSMO model output is used to investigate the interaction of Typhoon Jangmi (2008) with the midlatitude jet. The COSMO pseudo analysis indicated an acceleration of the jet stream and an increase of jet core wind speed when Jangmi approached the midlatitudes. After ET an extratropical cyclogenesis occurred downstream of Jangmi. Trajectory calculations along with selected cross sections of PV showed that Jangmi advects tropical moist air into the jet core along three distinct paths. An early ascent occurs in the vicinity of the PV tower associated with Jangmi. Most of the tropical air ascends at the eastern side of the tropical storm along a baroclinic zone that separates the subtropics from the midlatitudes. In the mid and upper levels air ascends along (moist) isentropes to jet level. Potential vorticity inversion along with modification of the PV field was used to quantify the impact of the tropical storm on the midlatitudes. A control run was initialized from the PV inversion on the original PV field and a NOTC run was computed from the PV inversion of a PV field in which Jangmi had been removed. The comparison of these two model runs showed that the outflow of Jangmi leads to an acceleration of the midlatitude jet and of the flow around the subtropical anticyclone. The PV surgery showed that Jangmi only has an impact on the intensity of the extratropical cyclogenesis which still occurs also when Jangmi is not present in the initial conditions.

REFERENCES

Agustí-Panareda, A., S. L. Gray, G. C. Craig, and C. Thorncroft, 2005: The Extratropical Transition of Tropical Cyclone Lili (1996) and Its Crucial Contribution to a Moderate Extratropical Development. *Monthly Weather Review*, **133**, 1562–+.

Agustí-Panareda, A., C. D. Thorncroft, G. C. Craig, and S. L. Gray, 2004: The extratropical transition of hurricane Irene (1999): A potential-vorticity perspective.
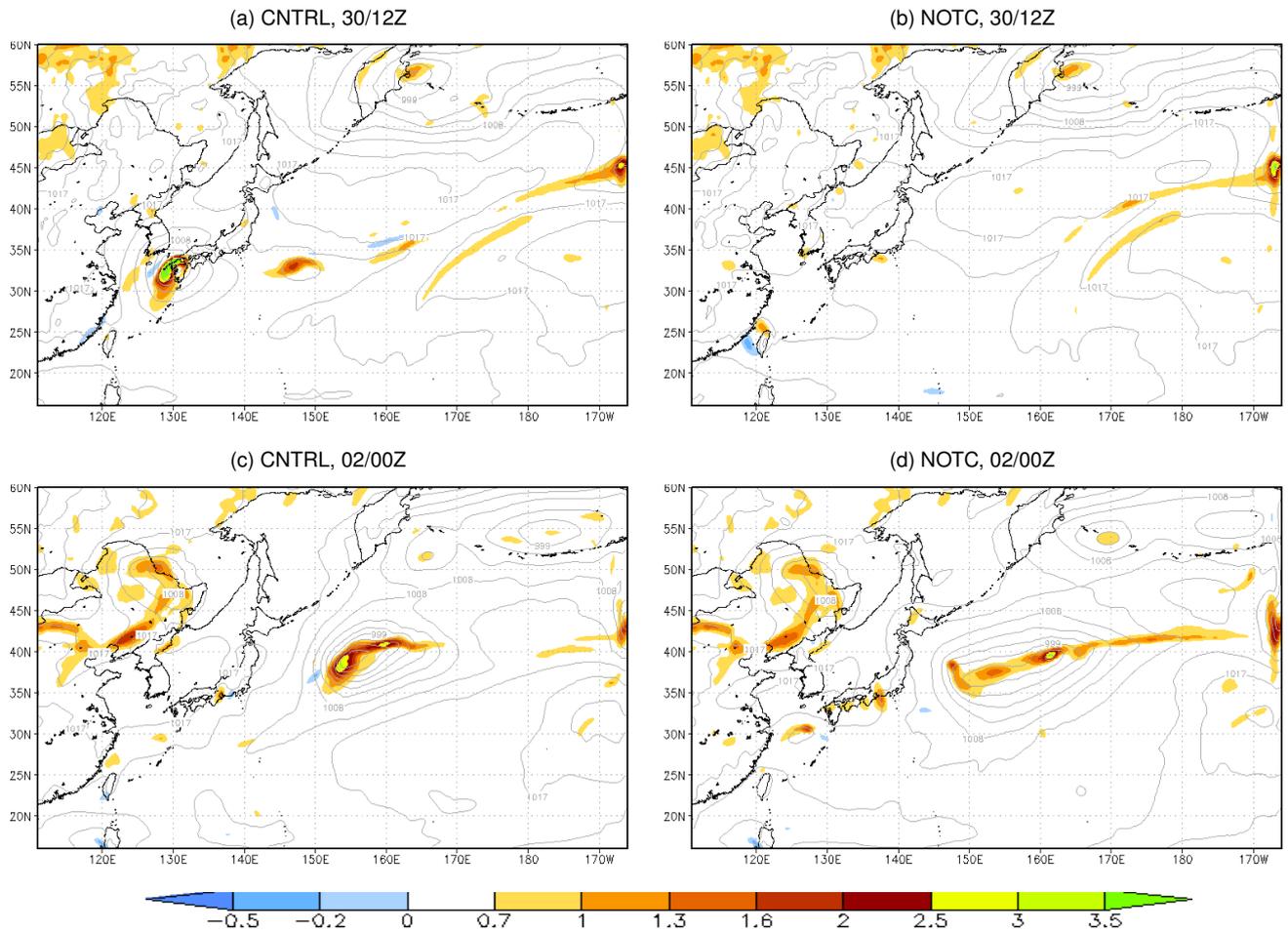
FIG. 8: Potential vorticity (shaded, in PVU) vertically averaged from 975-850 hPa, pressure at mean sea level (grey contours with a 4hPa contour interval), 12 UTC 30 September 2008 (top), and 00 UTC 02 October 2008 (bottom). Data in the left column is from CNTRL run, data in the right column is from NOTC run.

Quarterly Journal of the Royal Meteorological Society, **130**, 1047–1074.

Anwender, D., P. A. Harr, and S. C. Jones, 2008: Predictability Associated with the Downstream Impacts of the Extratropical Transition of Tropical Cyclones: Case Studies. *Monthly Weather Review*, **136**, 3226–+.

Charney, J. G., 1955: The use of primitive equations of motion in numerical prediction. *Tellus*, **7**, 22–26.

Davis, C. A., 1992: Piecewise Potential Vorticity Inversion. *Journal of Atmospheric Sciences*, **49**, 1397–1411.

Davis, C. A. and K. A. Emanuel, 1991: Potential Vorticity Diagnostics of Cyclogenesis. *Monthly Weather Review*, **119**, 1929–+.

Doms, G. and U. Schättler, 2002: A description of the nonhydrostatic Regional Model LM. Part I: Dynamics and Numerics. available at http://www.cosmo-model.org.

Ertel, H., 1942: Ein neuer hydrodynamischer Erhaltungssatz. *Meteorologische Zeitschrift*, **59**, 277–281.

Gaßmann, A., 2002: Numerische Verfahren in der nichthydrostatischen Modellierung und ihr Einfluss auf die Gte der Niederschlagsvorhersage. *Berichte des Deutschen Wetterdienstes*, **221**, 1–96.

Harr, P. A., D. Anwender, and S. C. Jones, 2008: Predictability Associated with the Downstream Impacts of the Extratropical Transition of Tropical Cyclones: Methodology and a Case Study of Typhoon Nabi (2005). *Monthly Weather Review*, **136**, 3205–+.

Kessler, E., 1969: On the distribution and continuity of water substance in atmospheric circulation models. *Meteorological Monographs*, **10**.

Klemp, J. B. and R. B. Wilhelmson, 1978: The Simulation of Three-Dimensional Convective Storm Dynamics. *Journal of Atmospheric Sciences*, **35**, 1070–1096.

Mellor, G. L. and T. Yamada, 1982: Development of a turbulence closure model for geophysical fluid problems. *Reviews of Geophysics and Space Physics*, **20**, 851–875.

Raschendorfer, M., 2001: The new turbulence parametrization of LM. *COSMO Newsletter*, **1**, 89–97.

Riemer, M., S. C. Jones, and C. A. Davis, 2008: The impact of extratropical transition on the downstream flow: An idealized modelling study with a straight jet. *Quarterly Journal of the Royal Meteorological Society*, **134**, 69–91.

Ritter, B. and J. F. Geleyn, 1992: A comprehensive radiation scheme for numerical weather prediction models with potential applications in climate simulations. *Monthly Weather Review*, **120**, 303–325.

Schättler, U., G. Doms, and C. Schraff, 2009: A description of the nonhydrostatic regional COSMO-model. Part VII: Userś Guide. available at http://www.cosmo-model.org.

Steppeler, J., G. Doms, U. Schättler, H. W. Bitzer, A. Gassmann, U. Damrath, and G. Gregoric, 2003: Meso-gamma scale forecasts using the nonhydrostatic model LM. *Meteorology and Atmospheric Physics*, **82**, 75–96.

Wernli, B. H. and H. C. Davies, 1997: A Lagrangian-based analysis of extratropical cyclones. I: The method and some applications. *Quarterly Journal of the Royal Meteorological Society*, **123**, 467–489.

Wernli, H., 1997: A Lagrangian-based analysis of extratropical cyclones. II: A detailed case-study. *Quarterly Journal of the Royal Meteorological Society*, **123**, 1677–1706.